

Sorting of Sphingolipids in Epithelial (Madin-Darby Canine Kidney) Cells

Gerrit van Meer, Ernst H. K. Stelzer, Roel W. Wijnaendts-van-Resandt, and Kai Simons

European Molecular Biology Laboratory, D-6900 Heidelberg, Federal Republic of Germany

Abstract. To study the intracellular transport of newly synthesized sphingolipids in epithelial cells we have used a fluorescent ceramide analog, *N*-6[7-nitro-2,1,3-benzoxadiazol-4-yl] aminocaproyl sphingosine (C6-NBD-ceramide; Lipsky, N. G., and R. E. Pagano, 1983, *Proc. Natl. Acad. Sci. USA*, 80:2608-2612) as a probe. This ceramide was readily taken up by filter-grown Madin-Darby canine kidney (MDCK) cells from liposomes at 0°C. After penetration into the cell, the fluorescent probe accumulated in the Golgi area at temperatures between 0 and 20°C. Chemical analysis showed that C6-NBD-ceramide was being converted into C6-NBD-sphingomyelin and C6-NBD-glucosylceramide. An analysis of the fluorescence pattern after 1 h at 20°C by means of a confocal scanning laser fluorescence microscope revealed that the fluorescent marker most likely concentrated in the Golgi complex itself. Little fluorescence was observed at the plasma membrane. Raising the temperature to 37°C for 1 h resulted in intense plasma membrane staining and a loss of fluorescence from the Golgi complex. Addition of BSA to the apical medium cleared the fluorescence from the apical but not from the basolateral plasma

membrane domain. The basolateral fluorescence could be depleted only by adding BSA to the basal side of a monolayer of MDCK cells grown on polycarbonate filters. We conclude that the fluorescent sphingomyelin and glucosylceramide were delivered from the Golgi complex to the plasma membrane where they accumulated in the external leaflet of the membrane bilayer. The results also demonstrated that the fatty acyl labeled lipids were unable to pass the tight junctions in either direction.

Quantitation of the amount of NBD-lipids delivered to the apical and the basolateral plasma membranes during incubation for 1 h at 37°C showed that the C6-NBD-glucosylceramide was two- to fourfold enriched on the apical as compared to the basolateral side, while C6-NBD-sphingomyelin was about equally distributed. Since the surface area of the apical plasma membrane is much smaller than that of the basolateral membrane, both lipids achieved a higher concentration on the apical surface. Altogether, our results suggest that the NBD-lipids are sorted in MDCK cells in a way similar to their natural counterparts.

IN an elegant series of papers Lipsky and Pagano (1983, 1985*a, b*) introduced the fluorescent ceramide analog, *N*-6[7-nitro-2,1,3-benzoxadiazol-4-yl] aminocaproyl sphingosine (C6-NBD-ceramide)¹ to study intracellular transport of sphingolipids. This ceramide partitions into tissue culture cells at 2°C and becomes trapped in the Golgi complex upon conversion to C6-NBD-sphingomyelin and *N*-6[7-nitro-2,1,3-benzoxadiazol-4-yl] aminocaproyl sphing-

osine glucoside (C6-NBD-glucosylceramide) at 37°C. These products then move to the plasma membrane from where they can be depleted by means of a "back exchange" reaction with unlabeled liposomes. In the present paper we have made use of these findings to study the sorting of lipids to the apical and basolateral membranes in epithelial cells.

Epithelial cells generally perform vectorial functions, which are reflected in the organization of their plasma membrane into an apical and a basolateral domain with unique lipid and protein compositions (see Rodriguez-Boulant, 1983; Simons and Fuller, 1985). The border between the domains is formed by the tight junction or zonula occludens, a structure that encircles the apex of each cell and links the individual cells together into epithelial monolayers. This tight junction is thought to prevent the intermixing of membrane components by forming a diffusion barrier in the plane of the membrane (Diamond, 1977; Simons and Fuller, 1985). We

G. van Meer's present address is Department of Cell Biology, Medical Faculty, State University of Utrecht, Nicolaas Beetsstraat 22, 3511 HG Utrecht, The Netherlands.

1. *Abbreviations used in this paper:* C6-NBD-ceramide, *N*-6[7-nitro-2,1,3-benzoxadiazol-4-yl] aminocaproyl sphingosine; C6-NBD-galactosylceramide, *N*-6[7-nitro-2,1,3-benzoxadiazol-4-yl] aminocaproyl sphingosine galactoside; C6-NBD-glucosylceramide, *N*-6[7-nitro-2,1,3-benzoxadiazol-4-yl] aminocaproyl sphingosine glucoside.

have recently provided evidence that the tight junction maintains the difference in lipid composition between the two domains by acting as a fence in the exoplasmic but not in the cytoplasmic leaflet of the plasma membrane bilayer (van Meer and Simons, 1986). The unique lipid compositions of the two domains can therefore be attributed to the compositions of the exoplasmic leaflet of each domain.

The presence of a barrier prevents intermixing of the apical and the basolateral lipids by lateral diffusion. However, the two domains are also connected by a vesicular route (see Mostov and Deitcher, 1986). To prevent equilibration of lipids via this route, separation of the two sets of lipids has to occur along the transcytotic pathway. This sorting event must involve a lateral segregation of some lipids into that part of the membrane which will bud into a transport vesicle, and exclusion of others from the bud. A similar sorting event has to occur along the biosynthetic pathway. Most lipids are synthesized in the endoplasmic reticulum and the Golgi complex (Pagano and Sleight, 1985). Newly synthesized lipids destined for the apical and the basolateral plasma membrane domains have to be physically separated during their transit from the endoplasmic reticulum and the Golgi complex to the plasma membrane. It is not known where in the transcytotic pathway the sorting occurs. In the biosynthetic pathway the *trans*-Golgi network (for a review see Griffiths and Simons, 1986) is emerging as a candidate for the site for sorting. Since the differences in lipid composition between the two plasma membrane domains seem to reside in the exoplasmic leaflet of the plasma membrane bilayer, it is reasonable to assume that sorting occurs in the exoplasmic, luminal leaflet of the membrane of the *trans*-Golgi network to generate the differences that are observed between apical and basolateral lipids.

Apical membranes have generally been found to be enriched in glycosphingolipids and sphingomyelin whereas phosphatidylcholine is concentrated in the basolateral domain (for a discussion see van Meer and Simons, 1986). Therefore the fluorescent sphingolipid C6-NBD-ceramide should serve as an excellent probe to study sorting of lipids to the apical surface in Madin-Darby canine kidney (MDCK) cells. Our strategy was to accumulate fluorescent analogs of the lipids in the Golgi complex using the observation that low temperature blocks traffic of membrane proteins from the Golgi complex to both the apical and the basolateral plasma membranes (Matlin and Simons, 1983; Pfeiffer et al., 1985). Upon release of the temperature "block" the cell surface appearance of the fluorescent lipids could be monitored both by confocal scanning laser fluorescence microscopy (Cox, 1984; Wijnaendts-van-Resandt et al., 1985) and through quantitative back exchange (Lipsky and Pagano, 1985a). We report here that the fluorescent analogs, C6-NBD-glucosylceramide and C6-NBD-sphingomyelin, are recognized by the cellular sorting machinery and seem to be sorted in a similar way as their native counterparts.

Materials and Methods

Lipids and Liposomes

C6-NBD-ceramide, C6-NBD-glucosylceramide, N-6[7-nitro-2,1,3-benzoxadiazol-4-yl] sphingosine galactoside (C6-NBD-galactosylceramide), and C6-NBD-sphingomyelin were synthesized from 6[7-nitro-2,1,3-benzoxadiazol-4-yl] aminocaproic acid (Molecular Probes, Inc., Junction City,

OR) and sphingosine, 1- β -D-galactosyl-sphingosine, 1- β -D-glucosyl-sphingosine, and sphingosylphosphoryl-choline, respectively (Sigma Chemical Co., St. Louis, MO), as described (Kishimoto, 1975). The products were quantitated spectrophotometrically in a fluorimeter (MPF-44A; Perkin-Elmer Corp., Norwalk, CT) with an excitation wavelength of 470 nm and emission measured at 535 nm, by comparison to a known amount of C6-NBD-phosphatidylethanolamine. Phospholipids were quantitated by a phosphate determination according to Rouser et al. (1970).

Small unilamellar liposomes were freshly prepared for each experiment from 435 nmol egg phosphatidyl choline (Sigma Chemical Co.) and 65 nmol C6-NBD-ceramide by octylglucoside dialysis (van Meer et al., 1985) in a final volume of 1 ml PBS (Dulbecco's formulation) and sonication by a probe sonicator at 70 W for 10 min in ice and under nitrogen. For some experiments 10^5 dpm of di[1- 14 C]palmitoyl phosphatidylcholine (112 Ci/mol; Amersham International, Amersham, United Kingdom) was incorporated into the liposomes as a tracer. Radioactivity was determined as described (van Meer et al., 1985). Before use the liposomes were diluted 1:2.5 (vol/vol) with Hanks' balanced salt solution (HBSS). Unlabeled liposomes consisting of egg phosphatidylcholine were prepared in the same way and used without dilution.

Lipid Analysis

Cellular lipids were extracted (Bligh and Dyer, 1959) and separated by two-dimensional high performance thin layer chromatography (HPTLC) as described (van Meer and Simons, 1982). The solvents used gave a clean separation of the fluorescent analogs of ceramide, free fatty acid, monoglycosyl ceramide, and sphingomyelin. In addition, C6-NBD-monoglycosyl ceramide was well separated from other fluorescent components of the cell culture media. In cell extracts C6-NBD-sphingomyelin ran as two partially overlapping spots. This appeared to be due to the underlying cellular sphingomyelin since pure C6-NBD-sphingomyelin ran as a single spot and addition of cellular lipids resulted in the double spot pattern. The reason for this is not clear. It is not due to fatty acid heterogeneity (Karlsson et al., 1973) because C6-NBD-sphingomyelin has C6-NBD-aminocaproic acid as its unique fatty acyl chain.

The C6-NBD-monoglycosylceramide was identified as C6-NBD-glucosylceramide by comparing its mobility on high performance thin layer plates with C6-NBD-galactosylceramide and C6-NBD-glucosylceramide standards. For this purpose lipids were run on borate impregnated or untreated thin layer plates (Kean, 1966) by a one-dimensional development in $\text{CHCl}_3/\text{CH}_3\text{OH}/4\text{ M NH}_4\text{OH}$ (65:35:5 vol/vol). For borate impregnation, a thin layer plate was sprayed with 50 ml of methanol containing 1.25 g boric acid. On treated and untreated plates the retention factors for the glucosylceramide (and the unknown monoglycosylceramide) were 2.4 and 1.4 times the retention factor of galactosylceramide, respectively. C6-NBD-glucosylceramide was the only NBD-glycolipid found in MDCK I and MDCK II cells.

After thin layer chromatography, fluorescent spots were scraped from the plate and extracted from the silica in 3.5 ml of a mixture of $\text{CHCl}_3/\text{CH}_3\text{OH}/\text{H}_2\text{O}$; 1:2.2:1. After pelleting the silica for 10 min at 1,500 g_{max} , the fluorescence intensity of the supernatant was determined as described above. The background values in such experiments were the following. When a cell extract was run on an HPTLC plate in the absence of NBD-lipids and when the ceramide spot was scraped from the plate, extracted, and measured, the value was equivalent to 2.8 ± 0.2 ($n = 5$) pmol NBD-lipid; for a glucosylceramide spot or sphingomyelin spot this was 0.8 ± 0.2 pmol. In the extract of 2.6 ml of HBSS the values were 2.3 ± 0.8 and 0.8 ± 0.3 pmol, respectively. HBSS without phenol red was used as an incubation medium in all experiments since phenol red and complete medium with or without serum gave rise to fluorescent spots on HPTLC plates, making the identification and quantitation of the NBD-lipids more difficult.

Cell Culture and Incubation Conditions

MDCK strain II cells were grown as 3-d-old monolayers on 0.45- μm pore size nitrocellulose acetate filters (Millipore filters; HATF 02500; Millipore SA, Molsheim, France) mounted in mini-Marbrook chambers (Hendley Engineering, Essex, UK) as described in detail (Matlin and Simons, 1984), or as 4-d-old monolayers on 0.4- μm pore size premounted polycarbonate filters (Transwell; Costar, Cambridge, MA). In the latter case the basolateral growth medium was replaced by fresh growth medium on day 3. A monolayer of MDCK II cells on Millipore filters (3.14 cm^2) contained 3.2×10^6 cells (Hansson et al., 1986). Monolayers of MDCK I and MDCK II on Transwells (4.5 cm^2) contained $(1.5 \pm 0.1) \times 10^6$ ($n = 3$) and $(2.4 \pm 0.1) \times 10^6$ ($n = 3$) cells, respectively. MDCK I cells grown on Millipore filters incorporated small amounts of C6-NBD-ceramide, and they were not used in the present study.

Monolayers on 20-mm-diam (Millipore) or 24.5-mm-diam (Transwell) filters were washed twice with HBSS and incubated for 30 min at 0 or 10°C with 500 (Millipore) or 750 μ l (Transwell) of C6-NBD-ceramide containing liposomes (26 nmol C6-NBD-ceramide/ml) on the apical side. After removal of the liposome suspension and two washes with HBSS, individual incubations were continued as described under Results. The applied amount of liposomes was saturating. The uptake of C6-NBD-ceramide by the cells did not increase when higher concentrations were used.

Unless indicated, the filters remained mounted in the chambers during all incubations. The mounted filters were situated in the wells of a 6-well plate (Nunc, Algaide, Denmark; Falcon Labware, Oxnard, CA; or in case of the polycarbonate filters, Costar) containing 4 or 2.6 ml of HBSS, respectively, while 1 ml of HBSS was present on the apical side of each filter. For incubations at 0°C the 6-well plates were modified so that the bottom of the wells rested directly on a metal plate on ice.

For back exchange (Lipsky and Pagano, 1985a) of NBD-lipids present on the cell surface a solution of 0.2% BSA (fraction V; Sigma Chemical Co.) in HBSS was added to the apical (1 ml) or basal (4 or 2.6 ml for Millipore or Transwell filters, respectively) side of the filter. Back exchange was performed during the 20°C incubation, during the 37°C incubation, or after the 37°C incubation at 0°C, as described in Results. When performed at 0°C the cells were incubated with BSA two times for 30 min. The first incubation released 87% of the C6-NBD-sphingomyelin and C6-NBD-glucosylceramide available for exchange, and the second incubation released a further 8%. During a subsequent incubation with media containing BSA or unlabeled liposomes, depletion increased by <5%. The addition of nonfluorescent liposomes to the BSA solution did not result in increased depletion. In experiments where cells were incubated with BSA at 37°C for shorter times than 20 min, this incubation was followed by a second one with BSA for 30 min at 0°C to complete the back exchange.

Fluorescence Microscopy

Conventional Fluorescence Microscopy. For screening purposes, cells on filters were viewed through a Zeiss photomicroscope III (Oberkochen, Federal Republic of Germany) by epifluorescence. A 40 \times water immersion objective was used to study living cells (van Meer and Simons, 1986).

Confocal Scanning Laser Microscopy. The resolution of the conventional fluorescence microscope along the optical axis is not sufficient to discriminate between the Golgi and the apical plasma membrane. Therefore, we applied a confocal scanning laser fluorescence microscope (Wijnaendts-van-Resandt et al., 1985). This microscope possesses true depth discrimination properties since only fluorescent light emitted in the plane of focus is detected. This is in contrast to a conventional fluorescence microscope, where light emitted by fluorophores outside the focal plane shows up as a diffuse background.

The configuration of the confocal scanning laser fluorescence microscope has been described in detail elsewhere (Marsman et al., 1983; Stelzer and Wijnaendts-van-Resandt, 1986). The instrument was used in the epifluorescence set up. The fluorophores in the sample were excited with the dark blue line (476 nm) of an argon ion laser. A dichroic LL50 Corion filter and parts of a Ploemopak (Ernst Leitz, Wetzlar, FRG) allowed only the fluorescent light emitted by the NBD-groups ($\lambda > 520$ nm) to enter the detector pinhole (≈ 200 μ m diam) and the photomultiplier (R 647; Hamamatsu Phototronics K. K., Hamamatsu City, Japan). The microscope was equipped with a Zeiss Axiomat ultrafluor 125 \times /1.25 Glyc objective, corrected for infinity, and the distance between lens and pinhole was 1,100 mm. The entrance aperture of the objective lens has a diameter of 4 mm. The diameter of the source pinhole was ≈ 100 μ m. It is important to realize that the optical path of the microscope remains fixed while the specimen is moved through the volume of the light spot, the size of which is diffraction limited. Electronic equipment drives the scanning movement in either a horizontal x/y - or a vertical x/z -plane, while a computer (VME-based 68000 microcomputer; Eltec, Mainz, FRG) monitors both the position of the light spot and the intensity detected by the photomultiplier. The intensity and the number of readings per picture element, pixel, are accumulated as a function of the position in the object. Due to the way the scan is performed, every pixel is read several times, on the average 16 times. The pixel values in the final image represent the mean of those 16 readings. During the scanning, the specimen is illuminated only as long as the fluorescent light is monitored. For this purpose the laser beam is switched on and off by means of an acousto-optic modulator. This deflection mechanism is coupled to the scanning movement.

Sample Preparation. Before microscopy monolayers of MDCK cells on Millipore filters were incubated according to one of the protocols described above and in the text. The filter was subsequently taken out of the holder and transferred to a petri dish on an ice-cold metal plate containing HBSS.

An 8-mm-diam piece was cut out from the filter with a punch. This piece of filter was placed in the center of a 22 \times 22 mm² coverslip and a drop of HBSS was applied to its apical surface. A small drop of dried nailpolish on each corner of the coverslip served as a spacer. A 20 \times 20 mm² coverslip was mounted atop of the spacers and the coverslips were sealed using nailpolish. The coverslip sandwich was subsequently mounted onto the table of the confocal scanning laser fluorescence microscope. This procedure made it possible to obtain the first images within 2 min after the sample had been removed from the ice-cold plate. Samples were viewed at temperatures below 20°C, no longer than 15 min after mounting.

Optical Sections. A first specimen was used to align the microscope and discarded. A fast scan in the x/y -plane with 256 lines/image, 70 lines/s and a field size of 174 \times 174 μ m² was then used to obtain an overview, to find the right areas and to move into the plane of interest. Images of horizontal optical sections were recorded in the x/y -plane with 1024 lines/image and 40 lines/s. The information of a set of four lines was combined to yield one row of pixels, resulting in the standard image of 256 \times 256 pixels. Focal series were recorded after defining the x/y -planes for the first and last image and the number of images in the series. The decrease in intensity caused while recording a series was determined by recording a second image in one of the x/y -planes and was found to be <10% of the total intensity in each plane of a series of 16 images at intervals along the z -axis of 1.2 μ m. For vertical optical sections (Wijnaendts-van-Resandt et al., 1985) a scan was performed in the x/z -plane with 512 lines/image and 40 lines/s. Lines were scanned parallel to the x -axis and again a set of four lines was combined to one row of pixels. In this case an image was obtained with 256 pixels in the x direction and 128 pixels in the z direction. Due to the microscope set up this image covered, at the magnification used, a field size of 76 μ m in the x direction and 54 μ m in the z direction. In the pictures of vertical sections shown in Figs. 2, 3, and 5 the scale along the z -axis has been normalized to that along the x -axis.

Images and Pictures. The high voltage supply of the photomultiplier tubes and the gain of the subsequent amplifier circuit had to be adapted to the available amount of light. Great care was taken that the analog-to-digital converter was operated in a correct range. As a consequence the intensity covered a window of ≈ 220 of the possible 256 grey levels. Images were stored in the computer. Pictures of the images were taken from a black and white monitor (FV 17; Knott Electr., Hoenschaftlarn, FRG) operated in interlace mode. A Minolta X-300 camera was attached to the monitor through an Oscilloscope M32A and an Oscillo-Quinon 5.6/55 mm lens. All pictures were recorded on 50 ASA Ilford Pan F film.

Quantitation. The amount of fluorophore was determined as a function of its localization in one of four categories: the apical plasma membrane, the basolateral plasma membrane, the Golgi area, and the cytosol. This was done by investigating six different cells in a focal series. Every pixel in a box covering the cell in all focal planes was classified as not belonging to this cell or as belonging to one of the categories mentioned above. The number of pixels and the sum of the intensities were recorded for each of the four categories and each plane. The division between the apical and basolateral plasma membrane was made arbitrarily as the plane in which the Golgi area was first detected when moving basal from the apical cell surface. In addition, the integrated intensity for the lateral membrane was divided by a factor of two, since this structure is formed by the lateral membranes of two neighboring cells in each case. The intensity ratios between different compartments varied by only 15% among the six different cells studied.

It has to be realized that the fluorescent signal registered by the microscope is the sum of the signals of the various NBD-containing lipids, since the microscope is unable to distinguish between single molecules. A limitation when using the microscope for quantitation is that at high concentrations of the fluorescent probe at a certain location, the relation between the signal of the microscope and the concentration of fluorescence may not be linear due to selfquenching. The concentration of fluorescent lipid in heavily labeled membranes may therefore be underestimated in microscopic images.

Information Content of an Image Obtained by Confocal Scanning Laser Microscopy. Every image obtained by the confocal scanning laser microscope consists of 256 \times 256 = 65,536 pixels, each capable of storing 256 grey levels. The intensity is linear with the pixel value. The lateral resolution in this configuration is <200 nm. With a field size of 76 \times 76 μ m² used for a typical picture, every pixel covers an area of 0.3 \times 0.3 μ m². The information in each pixel is therefore not influenced by the neighboring pixels. The resolution along the optical axis, defined as the distance from the fluorophore at which the intensity drops to 50% of its maximal value, is ≈ 1 μ m (Wijnaendts-van-Resandt et al., 1985). Images recorded in an x/z -plane therefore show "overlapping" information, while images recorded in a focal series at intervals of 1.2 μ m along the z -axis display independent in-

formation. Pictures of images obtained with the microscope necessarily lose the quantitative information, since it is not possible to print the 255 possible grey levels of such an image in the 40 grey tones of a photographic print. Such a picture therefore is the consequence of a selection of grey tones (and thereby contrast) by the photographer's eye.

Materials

Cell culture media were obtained from Gibco (Glasgow, UK). Chemicals and solvents were of analytical grade and obtained from Merck (Darmstadt, FRG).

Results

Cellular Uptake and Metabolic Conversion of C6-NBD-Ceramide

The aim of the initial experiments was to define the conditions under which MDCK cells would incorporate C6-NBD-ceramide and metabolize it to fluorescent glycolipid and sphingomyelin in the Golgi complex (Lipsky and Pagano, 1983, 1985a, b). To facilitate studies of transport to the plasma membrane we attempted to synchronize the delivery by accumulating the fluorescent lipids in the Golgi complex. Such an accumulation has been achieved for viral glycoproteins in MDCK cells by incubation of the cells at a reduced temperature of 20°C (Matlin and Simons, 1983). We therefore had the cells incorporate C6-NBD-ceramide from liposomes at 0°C to prevent endocytosis, washed away the liposomes, and continued the incubation for various times at 20°C before protein traffic to the cell surface was allowed to resume by warming to 37°C. In subsequent experiments 10°C was chosen instead of 0°C to increase the uptake of C6-NBD-ceramide by the cells.

Monolayers of MDCK II cells on Millipore filters were incubated with liposomes containing C6-NBD-ceramide on the apical side for 30 min at 0 or 10°C. The amount of C6-

NBD-ceramide that was incorporated by the cells was then quantitated by measuring the specific C6-NBD-ceramide uptake (Table I). Clearly more of the C6-NBD-ceramide became cell associated than of the liposome marker ¹⁴C-phosphatidylcholine. We conclude that this represented uptake of C6-NBD-ceramide into the cell by an exchange mechanism. After washing away the liposomes, the cells were further incubated at 20°C. During this incubation about half of the C6-NBD-ceramide was lost from the cells. This was accounted for by a release of liposomes that had been left attached to the cells after washing (Table I). After 30 min at 10°C followed by 1 h at 20°C, a total amount of 27 pmol NBD was present per 10⁶ MDCK II cells on Millipore filters, which is equivalent to 1.6 × 10⁷ fluorophores per cell. 85% of this had been taken up specifically by an exchange mechanism, while the remaining 15% could be accounted for by liposomes adhering to the cells. Since most likely part of this liposomal C6-NBD-ceramide partitioned into the cells during the subsequent 20°C incubation, the actual amount of NBD remaining at the apical cell surface in adhering liposomes was probably less than this 15%.

The metabolic conversion of C6-NBD-ceramide into C6-NBD-sphingomyelin and C6-NBD-glucosylceramide in MDCK II cells is illustrated in Fig. 1. C6-NBD-sphingomyelin and C6-NBD-glucosylceramide were rapidly produced in a ratio of ~5:1 following the shift to 20°C. The production of C6-NBD-sphingomyelin leveled off after 2 h and this was taken as a standard incubation time. If the temperature was raised to 37°C we noticed that some further metabolism occurred resulting in an increase of C6-NBD-sphingomyelin from 50 (Fig. 1) to 61% and of C6-NBD-glucosylceramide from 6 to 12% after 1 h. The rates and the extent of metabolism were identical on Millipore filters and on Transwells.

Since the continued conversion of C6-NBD-ceramide during the 37°C incubation might interfere with subsequent studies of cell surface appearance of the metabolic products,

Table I. Cell-associated C6-NBD-Ceramide*

Cell growth and incubation conditions	Total cell-associated C6-NBD-ceramide pmol/10 ⁶ cells (% of added)	Specific uptake of C6-NBD-ceramide† pmol/10 ⁶ cells (% of cell associated)
MDCK II cells on Millipore filters§		
0.5 h, 0°C	33 (0.81)	13 (39)
0.5 h, 0°C + 1 h 20°C	17 (0.43)	14 (82)
0.5 h, 10°C	58 (1.43)	24 (41)
0.5 h, 10°C + 1 h 20°C	27 (0.66)	23 (85)
MDCK I cells on Transwells		
0.5 h, 10°C	38 (0.29)¶	
MDCK II cells on Transwells		
0.5 h, 10°C	37 (0.45)¶	

* MDCK monolayers were incubated with C6-NBD-ceramide containing liposomes for 30 min at 0 or 10°C as described in Materials and Methods. 13 nmol C6-NBD-ceramide was added to 3.2 × 10⁶ MDCK II cells on a Millipore filter and 19.5 nmol C6-NBD-ceramide to 1.5 × 10⁶ MDCK I cells or 2.4 × 10⁶ MDCK II cells on Transwells. The filters were washed three times in HBSS, extracted or incubated for 1 h at 20°C in HBSS, and extracted. The extracts were divided into two equal parts. One part was used to determine the amount of C6-NBD-lipid by fluorescence spectrophotometry. The other part of the extract was dried under a stream of nitrogen in a scintillation vial and counted for the radioactivity of di[¹⁴C]palmitoyl phosphatidylcholine as a liposome marker. Both values were related to the amounts present in the original liposomes.

† Specific uptake represents the total amount of C6-NBD-ceramide, as quantitated by NBD fluorescence in the cells, minus the NBD fluorescence due to contaminating liposomes as quantitated by ¹⁴C radioactivity.

§ Three Millipore filters were used for each determination. Monolayers of MDCK II cells on Millipore filters contained 41 nmol phospholipid per 10⁶ cells (Hansson et al., 1986).

¶ Two Transwells were used for each determination. MDCK I: 37.7 ± 1.8 (n = 5) pmol/10⁶ cells (value followed by standard deviation and number of determinations in parentheses). This amount of NBD accounts for a mean number of 2.2 × 10⁷ fluorophores per cell. MDCK II: 36.7 ± 5.2 (n = 7) pmol/10⁶ cells, 2.1 × 10⁷ fluorophores per cell.

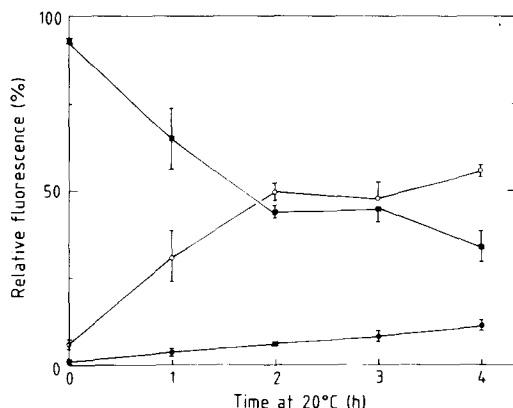


Figure 1. Cellular synthesis of C6-NBD-sphingomyelin (○) and C6-NBD-glucosylceramide (●) from C6-NBD-ceramide (■). Monolayers of MDCK II cells on Transwells were incubated with C6-NBD-ceramide containing liposomes for 30 min at 10°C, rinsed as described in Materials and Methods, and incubated at 20°C in HBSS. After varying time intervals two filters were cut out of their holders, their lipids extracted, and analyzed for fluorescent lipids. Each data point represents the mean of two pairs of Transwells. The error bar indicates the difference between the two measurements. After 1 h 100% equaled 21 pmol of NBD-lipid/ 10^6 cells, which remained constant during further incubation.

C6-NBD-ceramide metabolism was also assayed in MDCK I cells. Conversion was faster and more extensive in these cells. After 2 h at 20°C, $62 \pm 5\%$ ($n = 3$) of the total fluorescence was present as C6-NBD-sphingomyelin and $12 \pm 3\%$ ($n = 3$) as C6-NBD-glucosylceramide compared with 50 and 6% in MDCK II cells, respectively (Fig. 1). A more important difference was that the conversion of C6-NBD-ceramide in MDCK I cells did not continue during the following incubation at 37°C: after 1 h $62 \pm 4\%$ ($n = 5$) of the fluorescence was found in the sphingomyelin and $14 \pm 2\%$ ($n = 5$) in the glucosylceramide.

Intracellular Localization of C6-NBD-Sphingomyelin and C6-NBD-Glucosylceramide

Immediately after the incubation of the cells with liposomes containing C6-NBD-ceramide for 30 min at 0 or 10°C, a reticular staining was observed in every cell with a clear staining of the nuclear membrane (not shown; this staining could only be clearly discriminated in cells grown on a plastic support where the cells are much larger, 40 μ m diam, than when they are on Millipores, 12 μ m diam). Upon further incubation at 20°C this distribution changed drastically into the pattern shown in Fig. 2. The pictures were taken by a confocal scanning laser fluorescence microscope. This microscope has a resolution in the z direction of 1 μ m, which is far better than the conventional fluorescence microscope (Wijnaendts-van-Resandt et al., 1985). This true depth resolution makes it possible to view horizontal optical sections through the cells of <1 μ m thickness. In addition it is possible with this microscope to obtain vertical optical sections by recording images in an x/z -plane.

After 2 h at 20°C in HBSS most of the fluorescence accumulated in structures apical to the cell nucleus. The location in the MDCK cell and independent morphological evidence in other cell types (Lipsky and Pagano, 1983, 1985a, b) suggest that this structure is the Golgi complex. In addition to

the Golgi complex, an orthogonal network is faintly visible in Fig. 2 *b*. This represents the lateral plasma membranes of the cells. A fraction of the fluorescence was also observed in the cytoplasm, surrounding a dark spot near the base of the cell, the nucleus.

Production of C6-NBD-sphingomyelin also occurred at 10°C. After 3.5 h at 10°C, 34% of the NBD-fluorescence was present in this form. Since vesicular traffic in the cell is unlikely to proceed at this temperature (Dunn et al., 1980; Saraste and Kuismanen, 1984), it was important to find out where the C6-NBD-sphingomyelin would be localized under these conditions. Fig. 3 shows that fluorescence accumulated in the Golgi region. Fluorescence was also observed in the cytoplasm, while the nucleus was clearly devoid of fluorescence. Therefore production of sphingomyelin probably occurred in the Golgi complex (see Discussion).

Delivery of C6-NBD-Sphingomyelin and C6-NBD-Glucosylceramide at the Cell Surface

The distribution of the NBD fluorescence in the cell after

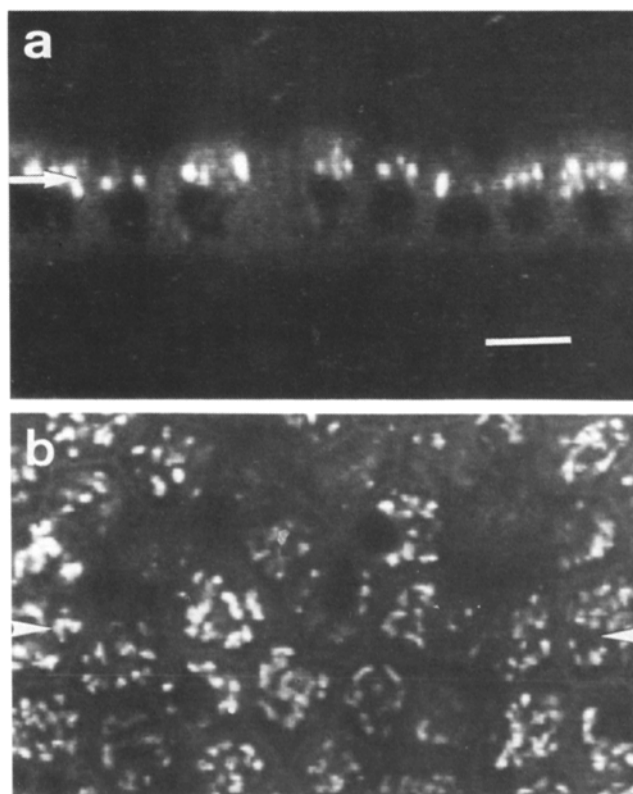


Figure 2. Localization of NBD fluorophores in the Golgi region of MDCK cells after 2 h at 20°C. Monolayers of MDCK II cells on Millipore filters were incubated with C6-NBD-ceramide containing liposomes for 30 min at 10°C as described in Materials and Methods. The cells were then incubated at 20°C for 2 h in HBSS after which they were viewed in a confocal scanning laser microscope. (a) Vertical optical section through the cell monolayer, generated as described under Materials and Methods. It has a thickness of <200 nm, the lateral resolution of the microscope. The arrow indicates the height at which the horizontal section (b) was taken. (b) Horizontal optical section 1 μ m thick through the cell monolayer. The arrowheads indicate the plane of the vertical section (a). Bar, 10 μ m.

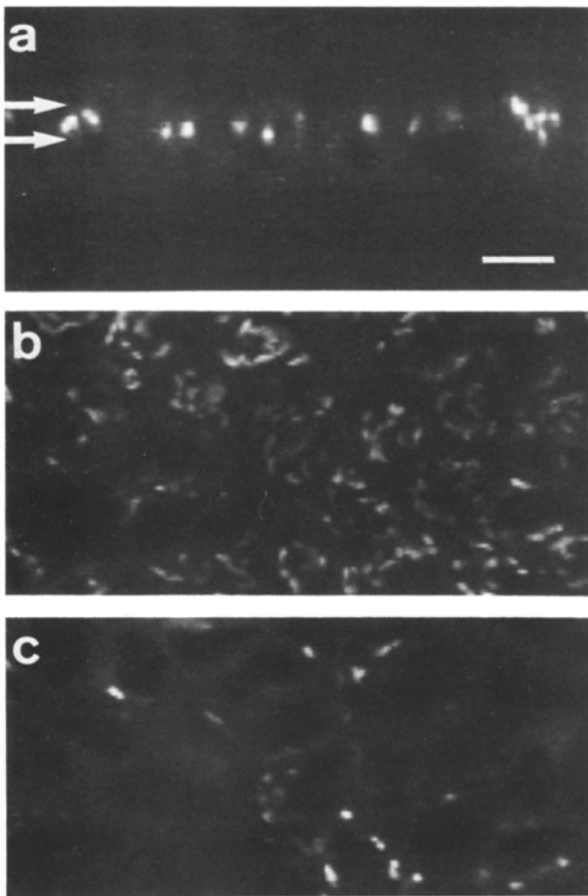


Figure 3. At 10°C NBD fluorescence concentrates in the Golgi area of the cell. MDCK II cells on Millipore filters were incubated at 10°C with C6-NBD-ceramide containing liposomes. After 30 min the liposomes were removed and the incubation continued at 10°C for 3.5 h in HBSS. At this time 34% of the C6-NBD-ceramide had been converted to C6-NBD-sphingomyelin. (a) Vertical optical section (as in Fig. 2 a) through a monolayer of cells. The arrows indicate the approximate location at which the horizontal sections *b* and *c* were taken, as in Fig. 2. The dark spots in *c* show that the nuclei do not contain fluorescence. Bar, 10 μ m.

2 h at 20°C changed rapidly when the cells were warmed to 37°C. Most of the label was present in the apical and basolateral plasma membrane after 1 h (Fig. 4). Only a small fraction of the fluorophores remained in the Golgi area. Hardly any fluorescence was observed in the cytoplasm. The fluorescence patterns in Fig. 4 are composed of the total fluorescence emitted by C6-NBD-sphingomyelin, C6-NBD-glucosylceramide, and C6-NBD-ceramide. The biochemical analysis of these cell monolayers showed that these three lipids contributed 61, 12, and 27% to the total fluorescence, respectively (see above). To quantitate the absolute amounts of the individual lipids that had reached the plasma membrane, we used the observation by Lipsky and Pagano (1985a)

that the fluorescent lipids on the cell surface can be removed by a back exchange reaction with unlabeled liposomes.

Adding a suspension of unlabeled liposomes to the apical side of cell monolayers like those shown in Fig. 4 for 30 min at 0°C caused loss of the fluorescence from the apical plasma membrane (Fig. 5). Incubation with HBSS containing 0.2% BSA had an identical effect (not shown). The fluorescence in the basolateral plasma membrane was not depleted by apically added liposomes or BSA. This made it possible to quantitate the fluorescence in the apical plasma membrane domain separately from that in the basolateral domain. The complementary quantitation requires a method to assay the fluorescent lipids from the basolateral domain. Depletion through the filter by incubation of the basal side of Millipore filters with unlabeled liposomes or BSA was unsuccessful. This was most likely due to the fact that the Millipore filters are ~ 100 μ m thick (10 times thicker than a monolayer of MDCK cells) and the "pores" are formed by the spaces in the network of nitrocellulose acetate fibers which show high nonspecific adsorption. We therefore tested a new type of permeable support for cell growth, Transwells (see Materials and Methods). These Transwells consist of premounted, "tissue culture-treated" polycarbonate filters of a thickness of only 10 μ m. In addition, the pores in Transwells are channels of a defined size.

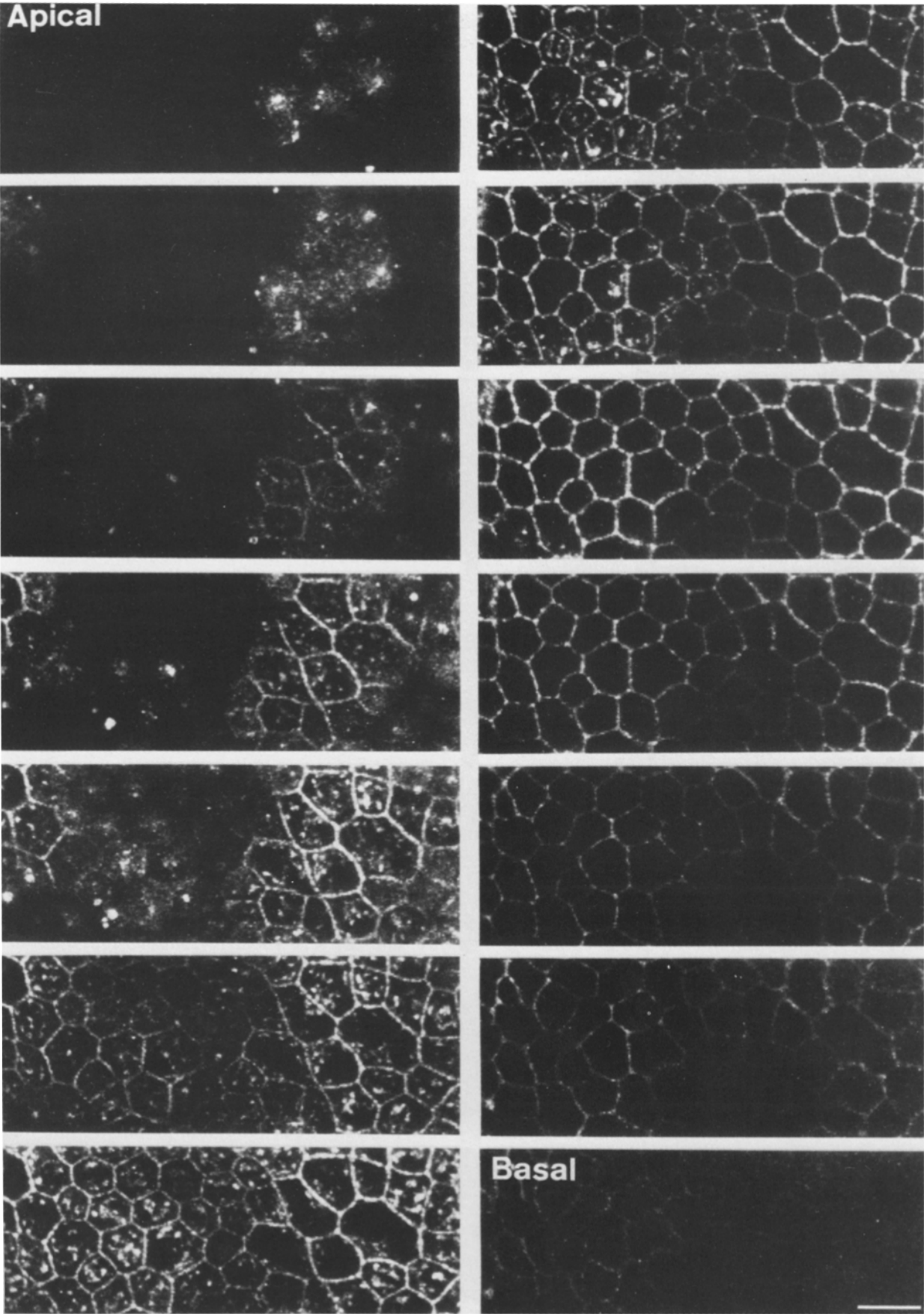
The application of BSA to the basal side of monolayers of MDCK cells on Transwells resulted in the complete removal of the fluorescence from the basolateral cell surface as monitored by the fluorescence microscope (not shown) and could be used to quantitate the fluorescent lipids present in the basolateral plasma membrane domain. The completeness of the back exchange process was controlled for all incubation conditions used. All fulfilled the criterion that subsequent incubations with BSA-containing HBSS should release <5% of additional C6-NBD-sphingomyelin or C6-NBD-glucosylceramide (see Materials and Methods). For this reason we used BSA-containing HBSS in all subsequent experiments.

C6-NBD-Sphingomyelin and C6-NBD-Glucosylceramide Polarity in MDCK Cells

To compare the amounts of C6-NBD-sphingomyelin and C6-NBD-glucosylceramide transported to the apical versus the basolateral plasma membrane domain at 37°C, the transport of the fluorescent lipid was first synchronized by an accumulation of the fluorescent lipid in the Golgi area at 20°C. During the incubation at 20°C, BSA was present on both surfaces of the filter to clear the plasma membrane of any products delivered at the surface during the 20°C accumulation step. At $t = 0$ the 20°C media were removed and replaced by fresh BSA-containing HBSS prewarmed to 37°C. The apical and basolateral media were collected at various times and the lipids in the cells and the media were analyzed. A typical experiment for MDCK I cells is shown in Fig. 6.

Immediately after the 20°C incubation, $60 \pm 1\%$ of the total cellular NBD-lipids consisted of C6-NBD-sphingomyelin

Figure 4. Intracellular distribution of NBD-fluorophores in MDCK cells after release from 20°C and 1 h at 37°C. NBD-lipids were concentrated in the Golgi area of MDCK II cells as described in the legend to Fig. 2, after which the cells were incubated for 1 h at 37°C in HBSS before being viewed in the microscope. Horizontal optical sections were recorded at 1.2- μ m intervals on the z-axis, from the apical (top left) towards the basal surface (bottom right) of the cell monolayer. For a vertical section through such a cell monolayer see Fig. 5 a. There is a bend in the cell monolayer. Therefore the apical surface of the cells to the right comes into focus first. Bar, 10 μ m.



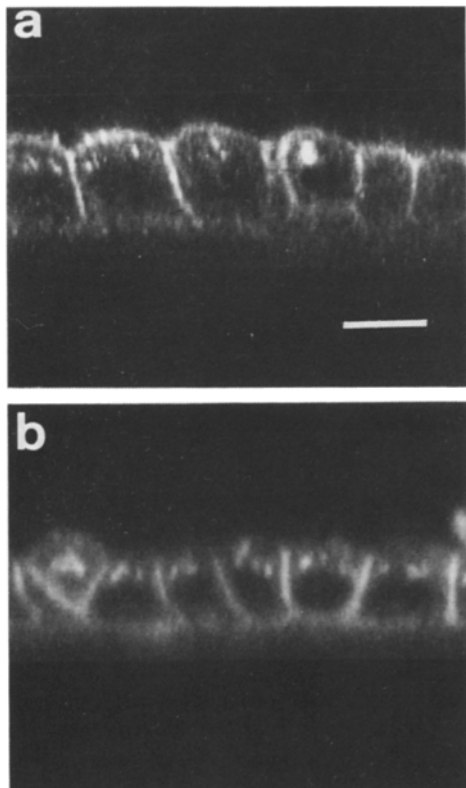


Figure 5. Depletion of apical fluorescence by the addition of unlabeled liposomes to the apical cell surface does not result in a depletion of NBD-lipids from the basolateral plasma membrane domain. (a) Vertical optical section (as in Fig. 2 a) through a monolayer of MDCK II cells treated as described in the legend to Fig. 4. (b) Parallel monolayers of cells were further incubated with unlabeled liposomes in HBSS on the apical surface for 30 min at 0°C (see Materials and Methods), after which they were viewed in the microscope. Bar, 10 μ m.

and $14 \pm 1\%$ of C6-NBD-glucosylceramide while the remaining 26% was still present as the precursor C6-NBD-ceramide. This ratio did not change during the 37°C incubation. In addition, no degradation of the NBD-sphingolipids to other C6-NBD-compounds occurred since the total amount of the three NBD-sphingolipids was constant throughout the experiment: 25 ± 2 pmol per 10^6 cells at $t = 0, 20, 40$, and 60 min. These numbers are about 30% lower than the amount of NBD-lipid that was cell associated after the 10°C incubation (37 pmol/ 10^6 cells). This is due to the loss of NBD-

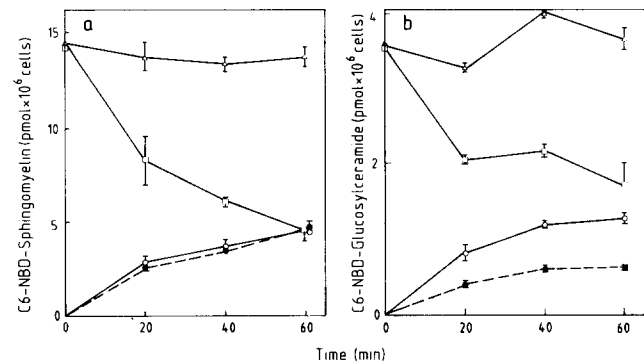


Figure 6. Appearance of C6-NBD-sphingomyelin (a) and C6-NBD-glucosylceramide (b) on the apical versus the basolateral plasma membrane of MDCK I cells at 37°C. Monolayers of MDCK I cells on Transwells were incubated with C6-NBD-ceramide containing liposomes for 30 min at 10°C. The incubation was continued for 2 h at 20°C in the absence of liposomes and the presence of 0.2% BSA in both apical and basolateral HBSS. At $t = 0$ the media on both sides were replaced by fresh BSA-containing HBSS prewarmed to 37°C. After different time intervals the media and the cells were analyzed for the presence of the individual fluorescent lipids. A typical experiment is shown. Parallel sets of four Transwells (2×2) each were used for individual time points. Total cell-associated NBD-lipids/ 10^6 cells after 30 minutes at 10°C: 36.5 ± 0.5 ($n = 2$) pmol; after the subsequent 2 h at 20°C: 24.7 ± 1.0 pmol. (\square) Intracellular; (\circ) apical; (\bullet) basolateral; (Δ) total (sum of the three other values). Each symbol represents the mean of two determinations, each of which was performed on two Transwells and normalized to 10^6 cells. The error bars show the difference between the two measurements.

lipids into the BSA-containing HBSS during the 20°C incubation (Tables I and III).

After the shift to 37°C, both C6-NBD-sphingomyelin (Fig. 6 a) and C6-NBD-glucosylceramide (Fig. 6 b) were transported to the cell surface with a $t_{1/2}$ of 20–30 min. About equal amounts of C6-NBD-sphingomyelin were delivered to the apical and basolateral plasma membrane domains. In contrast, two times more C6-NBD-glucosylceramide was transported to the apical than to the basolateral surface (Fig. 6 b; Table II).

The situation in MDCK II cells was similar but not identical to that in MDCK I cells (Fig. 7). About the same amounts of C6-NBD-sphingomyelin and C6-NBD-glucosylceramide were present in both cell types but in MDCK II cells, even after a 3-h instead of the usual 2-h incubation at 20°C (+BSA), $38 \pm 3\%$ ($n = 2$) of the total NBD-lipids were still

Table II. Polar Delivery of NBD-Sphingolipids to the Plasma Membrane of MDCK Cells during 1 h at 37°C*

Cell strain	Apical/basolateral†	
	C6-NBD-sphingomyelin	C6-NBD-glucosylceramide
MDCK I	1.07 ± 0.19 ($n = 8$)	2.10 ± 0.68 ($n = 8$)
MDCK II	0.87 ± 0.22 ($n = 25$)	2.58 ± 0.66 ($n = 14$)

* Cells were incubated as described in the legends to Figs. 6 and 7.

† The numbers represent the ratio between the absolute amounts of each fluorescent lipid available for back exchange from the apical and basolateral cell surfaces after incubations of 20, 40, or 60 min at 37°C. A pair of Transwells was used for each analysis. The mean of two pairs of Transwells was taken as one independent data point, e.g., the data of Fig. 6 contributed three data points to each column, as did the data of Fig. 7. The numbers are followed by the standard deviation and the number of data points.

Table III. Appearance of NBD-Sphingolipids at the Cell Surface during a 2-h 20°C Incubation*

Cell strain	C6-NBD-sphingomyelin [‡]		C6-NBD-glucosylceramide [‡]	
	Total cell surface	Apical/basolateral	Total cell surface	Apical/basolateral
	%		%	
MDCK I [§]	27.4 ± 5.5	(0.73 ± 0.43)	26.8 ± 5.2	(3.7 ± 2.0)
MDCK II	25.4 ± 2.5	(0.69 ± 0.09)	27.2 ± 1.2	(3.8 ± 0.9)

* Monolayers of MDCK cells on Transwells were incubated for 30 min at 10°C with C6-NBD-ceramide containing liposomes. After removal of the liposomes the monolayers were incubated at 20°C. BSA-containing HBSS was present on both the apical and the basolateral cell surface. After 2 h the apical and basolateral HBSS and the cells were extracted and the fluorescent lipids analyzed and quantitated as described in Materials and Methods. The total amounts of the NBD-lipids in cells plus media after the 20°C incubation were: 20 ± 3 pmol C6-NBD-sphingomyelin, 4 ± 1 pmol C6-NBD-glucosylceramide, and 14 ± 2 pmol C6-NBD-ceramide/10⁶ MDCK I cells. For MDCK II cells these numbers were 11 ± 1 pmol C6-NBD-sphingomyelin, 2.2 ± 0.4 pmol C6-NBD-glucosylceramide, and 23 ± 3 pmol C6-NBD-ceramide, respectively.

[‡] Numbers represent the percentage of each C6-NBD-lipid that was recovered from the combined apical and basolateral media after the 20°C incubation. They are followed by the standard deviation (*n* = 4). Two independent experiments were performed for each cell line. Two Transwells were analyzed for each data point. The numbers in parentheses indicate the ratio of apical to basolateral fluorophore.

[§] The standard deviations for these data are relatively high, probably because of the small amounts released. However, an excellent correlation existed between the individual experiments concerning the polarity of C6-NBD-glucosylceramide polarity as compared with that of C6-NBD-sphingomyelin; C6-NBD-glucosylceramide was 4.9 ± 0.8 (*n* = 4) times more enriched in the apical plasma membrane than C6-NBD-sphingomyelin.

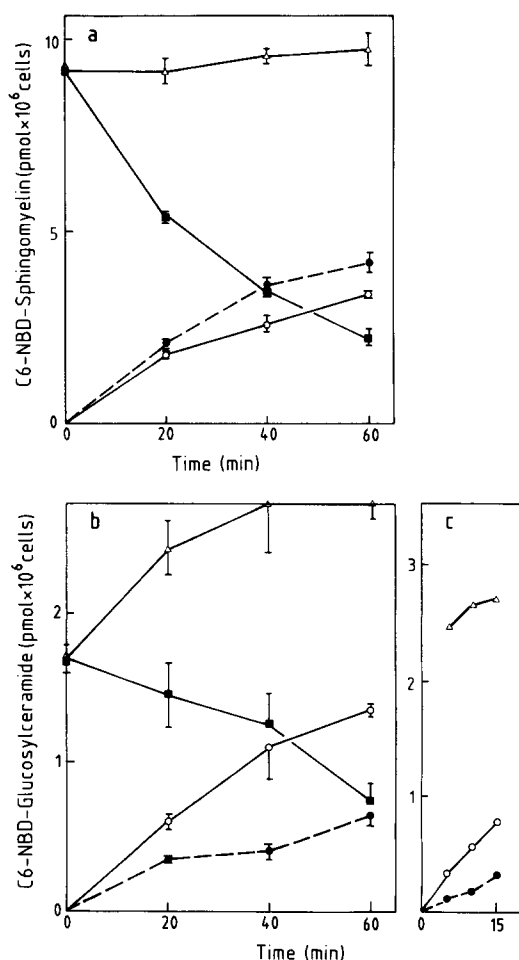


Figure 7. Appearance of C6-NBD-sphingomyelin (a) and C6-NBD-glucosylceramide (b and c) on the apical versus the basolateral plasma membrane of MDCK II cells at 37°C. Incubations and analyses were performed as in Fig. 6 for MDCK I cells, except for the fact that a 3-h incubation at 20°C was chosen instead of 2 h to accomplish a more complete conversion of C6-NBD-ceramide to its products. The results of a typical experiment are shown in a and b. (c) An independent experiment in which shorter time points were taken. After the 37°C incubation in c, fresh BSA-containing HBSS was added to both sides of the cell monolayer for another 0.5 h at

present as the C6-NBD-ceramide precursor as compared with 26% in MDCK I cells after 2 h. The synthesis of C6-NBD-glucosylceramide continued during the 37°C incubation. This resulted in a 50% increase in this lipid after 60 min. After the release from 20°C C6-NBD-sphingomyelin and C6-NBD-glucosylceramide appeared on the cell surface with half-times of 20–30 min as in MDCK I cells. Slightly more of the fluorescent sphingomyelin was delivered to the basolateral surface, while the C6-NBD-glucosylceramide was enriched over twofold in the apical plasma membrane (Table II). An experiment with short time intervals (Fig. 7 c) showed that the preferential delivery of C6-NBD-glucosylceramide to the apical surface occurred immediately after warming to 37°C. It is thus unlikely that the concentration on the apical side was a consequence of membrane recycling events.

As mentioned above, nearly 30% of the total C6-NBD-lipids in MDCK I cells and even 60% in MDCK II cells (Fig. 7) were released from the cells during the 20°C incubation with BSA. While in MDCK I cells about the same amounts of the individual NBD-lipids were present, in MDCK II cells the bulk of the released lipids was C6-NBD-ceramide. The leakage of fluorescent sphingomyelin and glucosylceramide to the cell surface was tested for polarity by back exchange experiments. The transport displayed equal or even higher polarity at 20°C than the transport at 37°C (Tables II and III).

0°C to achieve complete back exchange. After the experiment apical media and basolateral media were pooled separately and analyzed. Since the overall fluorescence in this experiment was slightly higher than in that shown in a and b, the scale of c was adapted to facilitate a comparison between the experiments. (a and b) Total cell-associated NBD-lipids/10⁶ cells after 30 min at 10°C: 39.0 ± 0.1 (*n* = 2) pmol; after the subsequent 3 h at 20°C: 16.2 ± 0.2 (*n* = 2) pmol. At 20°C mainly C6-NBD-ceramide was lost into the BSA-containing HBSS: 18.8 pmol. (●) Intracellular; (○) apical; (●) basolateral; (Δ) total (sum of the three other values). Each symbol represents the mean of two determinations, each of which was performed on two Transwells and normalized to 10⁶ cells. The error bars show the difference between the two measurements.

Morphometric data concerning the relative surface areas of the apical and basolateral plasma membrane domains are available for MDCK cells grown on Millipore filters (von Bonsdorff et al., 1985) but not for MDCK cells on Transwells. For this reason we also tried to quantitate the delivery of the C6-NBD-lipids to the cell surface of MDCK cells on Millipore filters. The BSA-depletion assay could not be used because it was not possible to clear the basolateral cell surface of NBD-lipids (see above). Instead, we used the confocal laser scanning microscope as described in Materials and Methods. In short, each pixel in the pictures of Fig. 4 (each panel is composed of roughly 256×96 pixels) has a relative intensity value between 0 and 255. By assigning each of the pixels to one of the four categories, basolateral plasma membrane, apical plasma membrane, Golgi area, and cytoplasm, and integrating the fluorescence values of those pixels, the following data were obtained. After the 37°C incubation, 77% of the fluorescent lipids were present in the plasma membrane, 10% in the Golgi area, and 13% in the cytoplasm. The ratio of apical to basolateral fluorescence was 0.64. At the same time, biochemical quantitation showed that $74 \pm 3\%$ ($n = 4$) of the NBD fluorescence was present as C6-NBD-sphingomyelin plus C6-NBD-glucosylceramide, and that depletion by BSA from the apical surface resulted in a release of $32 \pm 2\%$ ($n = 4$) of the total cellular C6-NBD-sphingomyelin after 1 h at 37°C. These numbers are very similar to the situation on Transwells, where 73% of the total NBD was present as C6-NBD-sphingomyelin and C6-NBD-glucosylceramide. On Transwells 77 and 73% of these lipids, respectively, were present in the plasma membrane and 35% of the C6-NBD-sphingomyelin could be depleted from the apical cell surface (Fig. 7).

C6-NBD-Sphingomyelin and C6-NBD-Glucosylceramide Do Not Diffuse between the Two Plasma Membrane Domains

Fig. 5 shows that removal of C6-NBD-lipids from the apical cell surface did not result in their depletion from the basolateral cell surface. This indicates that the C6-NBD-lipids are unable to diffuse from the basolateral to the apical cell surface. The complementary experiment, where the basolateral membrane was depleted of fluorescent lipids and the apical membrane monitored, was more difficult to interpret.

Although by eye no decrease in apical fluorescence was observed, a quantitative test was necessary to test if there was a change in the amount of NBD-lipids on the apical surface, or not. A biochemical assay was used to resolve this question.

Transwells with MDCK II cells were incubated as described in Fig. 7, but the BSA was present in the basolateral media only. After 1 h at 37°C the cells were cooled to 0°C and the media collected. Subsequently, fresh 0°C HBSS, this time containing BSA, was applied to the apical surface. The question was asked whether the fluorescent lipids that had been transported to the apical surface during the 20 and 37°C incubations would still reside there. As shown in Table IV the expected amounts of C6-NBD-sphingomyelin and C6-NBD-glucosylceramide were released from the apical cell surface by the subsequent incubation with the 0°C BSA-containing HBSS. About the same amount of C6-NBD-sphingomyelin was released into the 0°C apical HBSS as had been released into the 20 and 37°C basolateral media. Although the polarity of the C6-NBD-glucosylceramide was not quite as high as in the other experiments, most of it was found in the apical 0°C HBSS. The fluorescent lipids delivered to the apical surface remained there and were unable to pass the tight junction, just as the basolateral fluorescent lipids were prevented from diffusing into the apical surface in the earlier experiments.

Discussion

Our previous work has suggested that the tight junctions act as a diffusion barrier which maintains the differences in lipid composition between the apical and basolateral plasma membrane domains of MDCK cells (van Meer and Simons, 1986). In the present paper we have established an experimental system to study the generation of these lipid differences in the MDCK cell. We made use of the finding by Lipsky and Pagano (1983, 1985a, b) that cells can be manipulated to synthesize fluorescent sphingolipids, whose natural analogs appear to be enriched in the apical membrane of epithelial cells (see van Meer and Simons, 1986). The transport of the newly synthesized sphingolipids to both plasma membrane domains was then followed by quantitative methods.

Table IV. Basolateral BSA Does Not Deplete Apical C6-NBD-Lipids*

C6-NBD-lipid	Basolateral		Apical		Apical/basolateral†
	20°C	37°C	0°C, 0.5 h	0°C, 1 h	
C6-NBD-sphingomyelin	$1.54 \pm 0.04^{\S}$	2.27 ± 0.21	2.98 ± 0.17	0.46 ± 0.04	0.9
C6-NBD-glucosylceramide	0.10 ± 0.01	0.24 ± 0.03	0.48 ± 0.01	0.07 ± 0	1.6

* Monolayers of MDCK II cells on Transwells were incubated as described in the legend to Fig. 7, except that BSA was only on the basolateral side, and was absent from the apical media of the 20 and 37°C incubations. As in Fig. 7 the 37°C incubation was stopped after 1 h and the apical and basolateral media were collected for lipid analysis. However, here incubation was continued for 30 min at 0°C by the addition of fresh ice-cold HBSS, which this time contained BSA on both the apical and basolateral side of the cell monolayer. This protocol was repeated once. The apical media of the two subsequent 0°C incubations were termed apical 0°C, 0.5 h and apical 0°C, 1 h. After the experiment, altogether $69 \pm 2\%$ of the C6-NBD-sphingomyelin and $66 \pm 4\%$ of the glucosylceramide were recovered in the various media, the remainder, 3.26 and 0.46 pmol, respectively, still being present in the cells. Since the apical media of the 20 and 37°C incubations and the 0°C basolateral media did not contain any C6-NBD-sphingomyelin or C6-NBD-glucosylceramide fluorescence they were not included in the table.

† This column shows for each lipid the ratio of the fluorescence in the combined apical media (sum of columns 3 and 4) to the fluorescence in the combined basolateral media (sum of columns 1 and 2).

§ The numbers, pmol per 10^6 MDCK II cells, represent the mean of two pairs of Transwells (4.8×10^6 cells per pair) as in Fig. 7, and are followed by the difference of each measurement from the mean. The total amount of NBD-lipids per 10^6 cells in this experiment was lower than usual (18.7 ± 1.1 pmol).

Localization of the Metabolic Conversion

Upon presentation of C6-NBD-ceramide to MDCK cells at 0°C the fluorescent lipid immediately partitioned into the various cellular membranes as was reported for fibroblasts (Lipsky and Pagano, 1983, 1985a, b). C6-NBD-ceramide could therefore (at 0°C!) translocate across cellular membranes and exchange between membranes, through both the extra- and intracellular aqueous phase. Continued incubation at 20°C or below led to the accumulation of fluorophores in the Golgi area and to a concomitant production of C6-NBD-sphingomyelin and C6-NBD-glucosylceramide (Fig. 1). Under these conditions little fluorescent label was observed at the plasma membrane by microscopy (Figs. 2 and 3). Accumulation in the Golgi region was also observed at 10°C, at which temperature transport of proteins from the endoplasmic reticulum to the Golgi complex is blocked (Saraste and Kuismanen, 1984; Balch et al., 1986; Fries and Lindström, 1986).

Two important conclusions can be drawn from these observations. First, the majority of the fluorescent products is synthesized in the Golgi complex. Since over 80% of the products consisted of C6-NBD-sphingomyelin the conclusion is valid for this compound only. Previous studies using the ionophore monensin in fibroblasts have also led to the conclusion that C6-NBD-sphingomyelin is synthesized in the Golgi complex (Lipsky and Pagano, 1985a). This contrasts with reports in the recent literature that natural sphingomyelin is partially or exclusively synthesized at the plasma membrane (Voelker and Kennedy, 1982; Marggraf et al., 1982; van den Hill et al., 1985; Marggraf and Kanfer, 1987). The minor product, C6-NBD-glucosylceramide, cannot be localized by microscopy. The biochemical assays suggest that it is synthesized in a cellular compartment that is situated along a traffic route to the plasma membrane and located before the compartment of accumulation at 20°C in that pathway. Since the intracellular glycosyltransferases are preferentially located in the endoplasmic reticulum and the Golgi complex, these organelles are the main candidates for the site of synthesis of the glucosylceramide.

Second, since all C6-NBD-sphingolipids exchange between membranes at temperatures as low as 0°C, C6-NBD-ceramide is probably trapped in the Golgi complex by a metabolic conversion that is localized at the luminal surface of the Golgi membrane. This metabolic conversion must inhibit flip-flop of the C6-NBD-sphingolipids. Had they been able to move across the bilayer, both the C6-NBD-sphingomyelin and the C6-NBD-glucosylceramide should have been lost from the Golgi complex and partitioned into other cellular membranes. Direct evidence for a luminal location of the sphingolipids was obtained in the following way. When the apical plasma membrane of MDCK cells was perforated by shearing, the addition of BSA into the cytoplasm of the cells did not result in a depletion of fluorescent C6-NBD-sphingomyelin from the Golgi complex (Simons and Virta, 1987).

C6-NBD-Sphingomyelin and C6-NBD-Glucosylceramide Are Delivered to Both Plasma Membrane Domains and Are Unable to Pass the Tight Junction

The fluorescent label accumulated in both the apical and basolateral plasma membrane domains immediately after the release from 20°C (Figs. 4 and 5). We noticed that the apical

fluorescence was lost if the apical medium contained BSA and the lost C6-NBD-sphingolipids could be recovered from the medium (Lipsky and Pagano, 1985a, b). The depletion of the fluorescence from the apical cell surface by BSA appeared complete when monitored by microscopy (Fig. 5). Since the exchange reaction took place on the exoplasmic surface of the plasma membrane, all C6-NBD-sphingomyelin and C6-NBD-glucosylceramide in this membrane must have been present in the exoplasmic leaflet of the plasma membrane. We can exclude the possibility that a fraction of the C6-NBD-lipids was originally present in the cytoplasmic leaflets of the plasma membrane and then translocated to the outer leaflet during the exchange incubation. First, their presence in the cytoplasmic leaflet would have allowed the C6-NBD-sphingolipids to exchange to other intracellular membranes, which is not observed; under proper conditions fluorescence was observed exclusively at the plasma membrane with no fluorescent marker left in the Golgi complex. Second, if C6-NBD-lipids were present on the cytoplasmic side of the basolateral membrane, exchange through the cytoplasm and subsequent flip-flop in the apical plasma membrane would have led to their depletion from the basolateral plasma membrane domain as well. However, apical BSA depleted the fluorescence only from the apical and not from the basolateral surface (Fig. 5).

In the complementary experiment, C6-NBD-sphingomyelin and C6-NBD-glucosylceramide in the apical membrane could not be depleted by BSA present on the basolateral cell surface (Table IV). These findings agree with earlier work suggesting that gangliosides cannot diffuse across the tight junction (Spiegel et al., 1985), and with our own studies (van Meer and Simons, 1986), which showed that the fluorescent phospholipid *N*-(lissamine rhodamine-B-sulfonyl) phosphatidylethanolamine, having the fluorescent moiety on its polar head group, did not pass the tight junction from the apical to the basolateral cell surface when present in the exoplasmic leaflet of the plasma membrane. When it was situated in the cytoplasmic bilayer leaflet, the fluorescent lipid freely equilibrated across the tight junction, as had been suggested by work of Dragsten et al. (1981). All these results support the conclusion that the tight junction exerts its function as a fence for lipids in the outer half of the plasma membrane bilayer.

We conclude from these studies that both C6-NBD-sphingomyelin and C6-NBD-glucosylceramide are located in the exoplasmic, external leaflet of the plasma membrane of MDCK cells. Our earlier data (van Meer and Simons, 1986) suggested that phosphatidylcholine is also enriched in the exoplasmic leaflet of the plasma membrane of MDCK cells. In contrast, phosphatidylethanolamine was localized preferentially in the cytoplasmic leaflet. Thus the three major phospholipids in the MDCK cell plasma membrane tend to display the same *trans*-bilayer asymmetry as found in the membrane of the red blood cell (Verkley et al., 1973), which suggests that this asymmetry is a general property of plasma membranes. Less is known about the precise organization of glycolipids in membranes but the available evidence suggests that also glycolipids are localized in the exoplasmic leaflet of plasma membranes (Thompson and Tillack, 1985).

Lipid Sorting along the Biosynthetic Pathway

The characteristic differences in lipid composition between apical and basolateral plasma membrane domains are an en-

richment of glycolipids and, to a lesser extent, of sphingomyelin in the apical domain while phosphatidylcholine levels are always higher in the basolateral domain (for a discussion see van Meer and Simons, 1986). If C6-NBD-glucosylceramide (and C6-NBD-sphingomyelin) would mimic their cellular counterparts, they should be preferentially transported to the apical cell surface following biosynthesis. This was indeed the case.

Tables II and III and Figs. 6 and 7 show a preferential delivery of C6-NBD-glucosylceramide to the apical surface. Depending on the experiment, it was enriched two to five times as compared with the C6-NBD-sphingomyelin. However, these values do not reflect the full extent of sorting that takes place; the result of the sorting process is a differential surface concentration of the individual lipids on the two plasma membrane domains. Since the surface area of the apical domain is much smaller than that of the basolateral domain, equal absolute amounts of a certain lipid in each domain would result in a higher surface concentration of that lipid on the apical surface. The exact surface area values for MDCK cells grown on Transwells are not available yet. In contrast, detailed morphometric data are available for MDCK cells grown on Millipore filters (von Bonsdorff et al., 1985). Combining these values with the data that were obtained for the polarity of the C6-NBD-lipids at the cell surface of MDCK II cells grown on Millipore filters, we estimated that the cell surface concentration of the fluorescent products is >2.5 times higher on the apical plasma membrane. Since most of this fluorescence is C6-NBD-sphingomyelin, we conclude that also this sphingolipid is enriched in the apical plasma membrane, albeit to a lesser extent than C6-NBD-glucosylceramide. This apical enrichment of the fluorescent sphingolipids is not immediately clear from Fig. 5 *a*. The apical fluorescence per unit of plasma membrane length seems to be equal to that at the lateral surface. One has to realize, however, that the lateral staining is the sum of the fluorescence of the plasma membranes of two neighboring cells (and should therefore be divided by two). Furthermore, it cannot be excluded that the apical fluorescence is underestimated due to selfquenching (see Materials and Methods).

Our results suggest that C6-NBD-glucosylceramide and C6-NBD-sphingomyelin were preferentially delivered to the apical cell surface by vesicular transport from the Golgi complex. Synthesis at the plasma membrane seems unlikely; it is clear from the morphological studies that the appearance of the fluorescent lipids at the plasma membrane at 37°C was accompanied by a loss of fluorescence from the Golgi complex. Moreover, in MDCK I cells (Fig. 6) no synthesis of C6-NBD-sphingomyelin and C6-NBD-glucosylceramide occurred during the 37°C incubation. The localization of both fluorescent lipids in the luminal leaflet of the Golgi membrane and the exoplasmic leaflet of the plasma membrane argues that the transport of the fluorescent lipids between the two compartments occurred by means of carrier vesicles in which the NBD-lipids were located in the luminal bilayer leaflet. Whether those vesicles are the same ones that carry newly synthesized apical and basolateral proteins from the *trans*-Golgi to the respective surface domains remains to be shown. At least the rates of appearance of C6-NBD-sphingomyelin and C6-NBD-glucosylceramide closely resembled those measured for an apical membrane protein, the influ-

enza virus hemagglutinin (Matlin and Simons, 1984) and a basolateral protein, the vesicular stomatitis virus G protein (Pfeiffer et al., 1985) under similar experimental conditions. In addition, the polarized leak of the fluorescent lipids to the cell surface at 20°C (Table III) is of the same order as that of a membrane protein (Pfeiffer et al., 1985) and that of a secreted protein (Fries and Lindström, 1986).

The enrichment at the apical surface must have been due to direct delivery at the two surfaces and not a consequence of plasma membrane recycling because BSA was present on both cell surfaces throughout the experiments of Figs. 6 and 7. Sorting must therefore have occurred before the C6-NBD-lipids reached the plasma membrane. Had this not been the case, BSA would have trapped the lipids either apically or basolaterally. Analogous conclusions have been drawn concerning the sorting of membrane proteins in MDCK cells (Matlin and Simons, 1984; Misek et al., 1984; Pfeiffer et al., 1985; Caplan et al., 1986). It is also unlikely that the apical enrichment is due to a higher rate of membrane transport to the apical cell surface than to the basolateral surface. In that case the apical endocytic rate should be higher than that at the basolateral membrane in order to keep the surface areas of the two plasma membrane domains constant. This has not been observed. The apical and basolateral endocytic rates in MDCK cells per unit cell surface area are about equal (von Bonsdorff et al., 1985).

Lipid sorting involves the physical separation of two or more types of lipids. If we assume that lipids that have to be sorted are present in the luminal bilayer leaflet of an intracellular compartment, sorting must involve the lateral segregation in this leaflet of lipids into those areas of the membrane that will bud to form transport vesicles destined for either the apical or the basolateral plasma membrane domain. The factors involved in this segregation process are unknown. It should be emphasized that the lipids that are enriched in the apical membrane have a common feature, their sphingosine backbone, which is not present in the other membrane lipids. Moreover, these sphingolipids, especially the glycosphingolipids, have a tendency to associate by hydrogen bond formation to form separate domains in model lipid systems (Pascher, 1976; Thompson et al., 1986). The domain formation during sorting may be facilitated by the conditions in the lumen of the intracellular sorting compartment (e.g., low pH). Evidence is accumulating that suggests that sorting between apical and basolateral membrane proteins occurs in a late Golgi compartment, the *trans*-Golgi network (Griffiths and Simons, 1986; Matlin, 1986). The *trans*-Golgi network is also a good candidate for the site where the sorting between apical and basolateral sets of lipids occurs. It is hard to imagine that the two sorting processes would not be related. The finding that the two fluorescent lipids that we have used in this study, C6-NBD-sphingomyelin and C6-NBD-glucosylceramide, possess the structural requirements to be recognized by the cellular sorting machinery, opens new ways to study these sorting events in more detail.

We thank Thomas Gabran and Hilka Virta for excellent technical assistance. We are grateful to Jean Davoust and Stephen Fuller for critically reading the manuscript. The premounted and cell culture-treated Nuclepore filters (Transwell™) were kindly donated by Mr. Hank Lane of Costar, Cambridge, MA.

Received for publication 20 March 1987, and in revised form 4 June 1987.

References

- Balch, W. E., M. Elliott, and D. S. Keller. 1986. ATP-coupled transport of vesicular stomatitis virus G protein between the endoplasmic reticulum and the Golgi. *J. Biol. Chem.* 261:14681-14689.
- Bligh, E. G., and W. J. Dyer. 1959. A rapid method of total lipid extraction and purification. *Can. J. Biochem. Physiol.* 37:911-917.
- Caplan, M. J., H. C. Anderson, G. E. Palade, and J. D. Jamieson. 1986. Intracellular sorting and polarized cell surface delivery of (Na⁺,K⁺) ATPase, an endogenous component of MDCK cell basolateral plasma membranes. *Cell* 46:623-631.
- Cox, I. J. 1984. Scanning optical fluorescence microscopy. *J. Microsc. (Oxf.)* 133:149-154.
- Diamond, J. M. 1977. The epithelial junction: bridge, gate and fence. *Physiologist* 20:10-18.
- Dragsten, P. R., R. Blumenthal, and J. S. Handler. 1981. Membrane asymmetry in epithelia: is the tight junction a barrier to diffusion in the plasma membrane? *Nature (Lond.)* 294:718-722.
- Dunn, W. A., A. L. Hubbard, and N. N. Aronson, Jr. 1980. Low temperature selectively inhibits fusion between pinocytic vesicles and lysosomes during heterophagy of ¹²⁵I-asialofetuin by the perfused rat liver. *J. Biol. Chem.* 255:5971-5978.
- Fries, E., and I. Lindström. 1986. The effects of low temperatures on intracellular transport of newly synthesized albumin and haptoglobin in rat hepatocytes. *Biochem. J.* 237:33-39.
- Griffiths, G., and K. Simons. 1986. The trans Golgi network: sorting at the exit site of the Golgi complex. *Science (Wash. DC)* 234:438-443.
- Hansson, G. C., K. Simons, and G. van Meer. 1986. Two strains of the Madin-Darby canine kidney (MDCK) cell line have distinct glycosphingolipid compositions. *EMBO (Eur. Mol. Biochem. Organ.) J.* 5:483-489.
- Karlsson, K.-A., B. E. Samuelsson, and G. O. Steen. 1973. The sphingolipid composition of bovine kidney cortex, medulla and papilla. *Biochim. Biophys. Acta* 316:317-335.
- Kean, E. L. 1966. Separation of gluco- and galactocerebrosides by means of borate thin-layer chromatography. *J. Lipid Res.* 7:449-452.
- Kishimoto, Y. 1975. A facile synthesis of ceramides. *Chem. Phys. Lipids* 15:33-36.
- Lipsky, N. G., and R. E. Pagano. 1983. Sphingolipid metabolism in cultured fibroblasts: microscopic and biochemical studies employing a fluorescent ceramide analogue. *Proc. Natl. Acad. Sci. USA* 80:2608-2612.
- Lipsky, N. G., and R. E. Pagano. 1985a. Intracellular translocation of fluorescent sphingolipids in cultured fibroblasts: endogenously synthesized sphingomyelin and glucocerebroside analogues pass through the Golgi apparatus en route to the plasma membrane. *J. Cell Biol.* 100:27-34.
- Lipsky, N. G., and R. E. Pagano. 1985b. A vital stain for the Golgi apparatus. *Science (Wash. DC)* 228:745-747.
- Marggraf, W.-D., and J. N. Kanfer. 1987. Kinetic and topographical studies of the phosphatidylcholine:ceramide cholinephosphotransferase in plasma membrane particles from mouse ascites cells. *Biochim. Biophys. Acta* 897:57-68.
- Marggraf, W. D., R. Zertani, F. A. Anderer, and J. N. Kanfer. 1982. The role of endogenous phosphatidylcholine and ceramide in the biosynthesis of sphingomyelin in mouse fibroblasts. *Biochim. Biophys. Acta* 710:314-323.
- Marsman, H. J. B., G. J. Brakenhoff, P. Blom, R. Stricker, and R. W. Wijnaendts-van-Resandt. 1983. Mechanical scan system for microscopic applications. *Rev. Sci. Instrum.* 54:1047-1052.
- Matlin, K. S. 1986. The sorting of proteins to the plasma membrane in epithelial cells. *J. Cell Biol.* 103:2565-2568.
- Matlin, K. S., and K. Simons. 1983. Reduced temperature prevents transfer of a membrane glycoprotein to the cell surface but does not prevent terminal glycosylation. *Cell* 34:233-243.
- Matlin, K. S., and K. Simons. 1984. Sorting of an apical plasma membrane glycoprotein occurs before it reaches the cell surface in cultured epithelial cells. *J. Cell Biol.* 99:2131-2139.
- Misek, D. E., E. Bard, and E. Rodriguez-Boulant. 1984. Biogenesis of epithelial cell polarity: Intracellular sorting and vectorial exocytosis of an apical plasma membrane glycoprotein. *Cell* 39:537-546.
- Mostov, K. E., and D. L. Deitcher. 1986. Polymeric immunoglobulin receptor expressed in MDCK cells transcytoses IgA. *Cell* 46:613-621.
- Pagano, R. E., and R. G. Sleight. 1985. Emerging problems in the cell biology of lipids. *Trends Biochem. Sci.* 10:421-425.
- Pascher, I. 1976. Molecular arrangements in sphingolipids. Conformation and hydrogen bonding of ceramide and their implication on membrane stability and permeability. *Biochim. Biophys. Acta* 455:433-451.
- Pfeiffer, S., S. D. Fuller, and K. Simons. 1985. Intracellular sorting and basolateral appearance of the G protein of vesicular stomatitis virus in Madin-Darby canine kidney cells. *J. Cell Biol.* 101:470-476.
- Rodriguez-Boulant, E. 1983. Membrane biogenesis, enveloped RNA viruses, and epithelial polarity. In *Modern Cell Biology*. Vol. 1. B. H. Satir, editor. Alan R. Liss, Inc., New York. 119-170.
- Rouser, G., S. Fleischer, and A. Yamamoto. 1970. Two-dimensional thin-layer chromatographic separation of polar lipids and determination of phospholipids by phosphorus analysis of spots. *Lipids* 5:494-496.
- Saraste, J., and E. Kuismanen. 1984. Pre- and post-Golgi vacuoles operate in the transport of Semliki Forest virus membrane glycoproteins to the cell surface. *Cell* 38:535-549.
- Simons, K., and S. D. Fuller. 1985. Cell surface polarity in epithelia. *Annu. Rev. Cell Biol.* 1:243-288.
- Simons, K., and H. Virta. 1987. Perforated MDCK cells support intracellular transport. *EMBO (Eur. Mol. Biochem. Organ.) J.* 6:2241-2247.
- Spiegel, S., Blumenthal, R., Fishman, P. H., and J. S. Handler. 1985. Gangliosides do not move from apical to basolateral plasma membrane in cultured epithelial cells. *Biochim. Biophys. Acta* 821:310-318.
- Stelzer, E. H., and R. W. Wijnaendts-van-Resandt. 1986. Applications of fluorescence microscopy in three dimensions: microtomography. *Proc. S.P.I.E.* 602:63-70.
- Thompson, T. E., and T. W. Tillack. 1985. Organization of glycosphingolipids in bilayers and plasma membranes of mammalian cells. *Annu. Rev. Biophys. Chem.* 14:361-386.
- Thompson, T. E., Y. Barenholz, R. E. Brown, M. Correa-Freire, W. W. Young, and T. W. Tillack. 1986. Molecular organization of glycosphingolipids in phosphatidylcholine bilayers and biological membranes. In *Enzymes of Lipid Metabolism*. L. Preys, editor. Plenum Publishing Corp., New York. 387-396.
- van den Hill, A., G. P. H. van Heusden, and K. W. A. Wirtz. 1985. The synthesis of sphingomyelin in the Morris hepatomas 7777 and 5123D is restricted to the plasma membrane. *Biochim. Biophys. Acta* 833:354-357.
- van Meer, G., and K. Simons. 1982. Viruses budding from either the apical or the basolateral plasma membrane domain of MDCK cells have unique phospholipid compositions. *EMBO (Eur. Mol. Biochem. Organ.) J.* 1:847-852.
- van Meer, G., and K. Simons. 1986. The function of tight junctions in maintaining differences in lipid composition between the apical and basolateral cell surface domains of MDCK cells. *EMBO (Eur. Mol. Biochem. Organ.) J.* 5:1455-1464.
- van Meer, G., J. Davoust, and K. Simons. 1985. Parameters affecting low-pH-mediated fusion of liposomes with the plasma membrane of cells infected with influenza virus. *Biochemistry* 24:3593-3602.
- Verkley, A. J., R. F. A. Zwaal, B. Roelofs, P. Comfurius, D. Kastelijn, and L. L. M. van Deenen. 1973. The asymmetric distribution of phospholipids in the human red cell membrane. A combined study using phospholipases and freeze-etch electron microscopy. *Biochim. Biophys. Acta* 323:178-193.
- Voelker, D. R., and E. P. Kennedy. 1982. Cellular and enzymic synthesis of sphingomyelin. *Biochemistry* 21:2753-2759.
- von Bonsdorff, C.-H., S. D. Fuller, and K. Simons. 1985. Apical and basolateral endocytosis in Madin-Darby canine kidney (MDCK) cells grown on nitrocellulose filters. *EMBO (Eur. Mol. Biochem. Organ.) J.* 4:2781-2792.
- Wijnaendts-van-Resandt, R. W., H. J. B. Marsman, R. Kaplan, J. Davoust, E. H. K. Stelzer, and R. Stricker. 1985. Optical fluorescence microscopy in three dimensions: microtomography. *J. Microsc. (Oxf.)* 138:29-34.